Available online at www.sciencedirect.com
SCIENCE DIRECT
Journal of Power Sources 155 (2006) 447–455
JOURNAL OF POWER SOURCES
www.elsevier.com/locate/jpowsour

Dehydriding reactions of mixed complex hydrides

Y. Nakamori [a], A. Ninomiya [a], G. Kitahara [a], M. Aoki [b], T. Noritake [b], K. Miwa [b], Y. Kojima [b], S. Orimo [a,*]

[a] *Institute for Materials Research, Tohoku University, Sendai 980-8577, Japan*
[b] *Toyota Central R&D Labs. Inc., Nagakute, Aichi 480-1192, Japan*

Received 15 February 2005; received in revised form 3 April 2005; accepted 3 April 2005
Available online 13 June 2005

Abstract

Dehydriding reactions of the mixtures $LiBH_4 + 2LiNH_2$ and $LiAlH_4 + 2LiNH_2$ were investigated. The new pathways confirmed for the dehydriding reactions were $LiBH_4 + 2LiNH_2 \rightarrow Li_3BN_2 + 4H_2$ and $LiAlH_4 + 2LiNH_2 \rightarrow Li_3AlN_2 + 4H_2$ in which 11.9 and 9.6 mass% of hydrogen can be desorbed theoretically. The quantities of desorbed hydrogen were deduced experimentally to be approximately 7.9–9.5 and 4.1 mass% for the mixtures of $LiBH_4 + 2LiNH_2$ and $LiAlH_4 + 2LiNH_2$, respectively. The dehydriding temperature of $LiBH_4$ reduces by 150 K by mixing 2 M $LiNH_2$. An exothermic peak was observed at a slightly higher temperature of the dehydriding reaction; however, this peak might be due to the solidification of the product after the dehydriding reaction and not due to the exothermic dehydriding reaction. Although the first-step dehydriding reaction of $LiAlH_4$ is exothermic, the mixture of $LiAlH_4 + 2LiNH_2$ exhibits an endothermic dehydriding reaction. These results suggest that the stability of the dehydriding reactions of complex hydrides can be controlled by introducing new pathways that are produced by mixing. Two criteria for selecting complex hydrides that are mixed together for producing new pathways were proposed from the viewpoints of both the melting/dehydriding temperatures and the products of the dehydriding reactions.

Keywords: Complex hydrides; Lithium; Borohydride; Amide; Boronitride; Hydrogen storage

1. Introduction

Hydrogen has attracted considerable attention as a new energy carrier in order to realise clean and environment-friendly energy systems. For this purpose, hydrogen storage materials with high hydrogen densities (greater than 5–6 mass%) and low dehydriding temperatures (below 373–423 K) are being developed extensively.

One of the candidates for hydrogen storage materials is the complex hydride. For example, $LiBH_4$ and $LiAlH_4$ desorb hydrogen as follows:

$$LiBH_4 \rightarrow LiH + B + (3/2)H_2 \quad (1)$$

$$LiAlH_4 \rightarrow (1/3)Li_3AlH_6 + (2/3)Al + H_2 \rightarrow LiH + Al + (3/2)H_2 \quad (2)$$

According to Eq. (1), $LiBH_4$ desorbed more than 13.8 mass% of hydrogen, and the dehydriding temperature was reported to be above 600 K [1]. This temperature is much higher than that desired, particularly for polymer–electrode fuel cells. On the other hand, $LiAlH_4$ desorbed 5.3 and 2.7 mass% of hydrogen, and the dehydriding temperatures for the first- and second-step reactions of Eq. (2) were reported to be approximately 400 and 500 K, respectively [2]. However, the first- and second-step dehydriding reactions are exothermic and endothermic, respectively. This hinders the rehydriding (absorbing) reaction of the $LiAlH_4$ system.

With the exception of the hydrolysis reaction of borohydrides [3,4], the dehydriding reactions of complex hydrides,

* Corresponding author. Tel.: +81 22 215 2093; fax: +81 22 215 2091.
E-mail address: orimo@imr.tohoku.ac.jp (S. Orimo).

0378-7753/$ – see front matter © 2005 Elsevier B.V. All rights reserved.
doi:10.1016/j.jpowsour.2005.04.013

such as $MM'H_4$ (M = Li, Na, K and Mg; and M' = B and Al), have been investigated typically from the viewpoint of their 'decomposition' [5–10], similar to Eqs. (1) and (2). In this case, the effective control of the dehydriding reaction appears to be limited because the reaction predominantly depends on the stability of the complex hydride.

It has been reported that Li_3NH_4 (a mixture of $LiNH_2$ and 2LiH) proceeds with the partial dehydriding reaction [11]. Recently, Chen et al. have focused on the dehydriding reaction of the mixture of $LiNH_2$ and 2LiH (or LiH) as a hydrogen storage material for fuel cell applications [12]. The dehydriding reaction is expressed as follows:

$$LiNH_2 + 2LiH \leftrightarrow Li_2NH + LiH + H_2 \leftrightarrow Li_3N + 2H_2 \quad (3)$$

In the first- and second-step reactions, 5.5 and 5.2 mass% of hydrogen can be desorbed at approximately 470 and 700 K, respectively. It is interesting to compare the dehydriding reaction of each material, $LiNH_2$ and LiH, with that of the mixture of $LiNH_2$ + LiH in Eq. (3). $LiNH_2$ decomposes into Li_2NH and NH_3 at approximately 573 K with increasing temperatures [13]. LiH desorbs more than 12 mass% of hydrogen; however, the dehydriding temperature is higher than the melting temperature of 953 K [14]. On the other hand, the mixture of $LiNH_2$ + LiH desorbs only hydrogen [13] even at temperature lower than the dehydriding temperature of LiH. These experimental results indicate that complex hydrides, which do not desorb hydrogen under desired conditions, proceed with the dehydriding reaction under appropriate conditions by producing a new pathway in the mixtures with other hydrides.

In this study, we focus on the mixture of the complex hydrides of $LiBH_4 + LiNH_2$ and that of $LiAlH_4 + LiNH_2$. The expected new pathways for the dehydriding reactions are

$$LiBH_4 + 2LiNH_2 \rightarrow Li_3BN_2 + 4H_2 \quad (4)$$

$$LiAlH_4 + 2LiNH_2 \rightarrow Li_3AlN_2 + 4H_2 \quad (5)$$

A total of 11.9 and 9.6 mass% of hydrogen are predicted to be desorbed in Eqs. (4) and (5), respectively.

Fig. 1 schematically shows the enthalpy changes ΔH of the dehydriding reactions of Eqs. (1) and (3) deduced from the experiments and that of Eq. (4) predicted from the first-principles calculations performed by the ultrasoft pseudopotential method [17] on the basis of the density-functional theory [18]. The generalised gradient approximation was used for the exchange-correlation energy [19]. The computational details are shown in ref. [20].

The values of ΔH and the entropy changes ΔS at a temperature T K are expressed by the van't Hoff equation [21]:

$$\ln(p_{eq}/p^0_{eq}) = (\Delta H/RT) - (\Delta S/R) \quad (6)$$

Here, p_{eq} is the equilibrium pressure, p^0_{eq} the standard pressure of 0.1 MPa and R is the gas constant. Assuming that

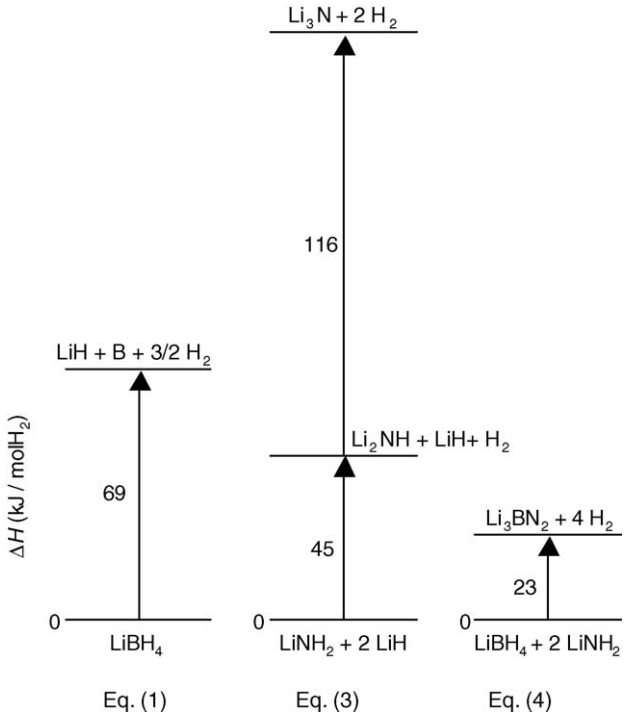

Fig. 1. Enthalpy changes ΔH for the dehydriding reactions of $LiBH_4$ [15] (Eq. (1)), the mixture of $LiNH_2$ + 2 LiH [12] (Eq. (3)) deduced from the experiments, and that for the mixture of $LiBH_4 + 2LiNH_2$ (Eq. (4)) predicted from the first-principles calculations [16].

ΔS equals 130 J mol^{-1} K^{-1}, since the entropy changes from the hydrogen molecule to the hydrogen atom dissolved in the solid state system, ΔH was deduced to be 19.6 kJ mol H_2 for the desired dehydriding reaction at 300 K under 0.1 MPa of hydrogen. However, ΔH for the dehydriding reaction of $LiBH_4$ is 69 kJ mol H_2, which proves to be extremely stable for practical applications at 300 K under 0.1 MPa. On the other hand, ΔH for the dehydriding reaction of the mixture of Eq. (4) is predicted from Eq. (6) to be 23 kJ mol H_2, which is appropriate for the dehydriding reaction at room temperature under 0.1 MPa of hydrogen from Eq. (6).

Promoted by the prediction, the actual dehydriding reaction of the mixture of $LiBH_4 + LiNH_2$ (Eq. (4)) is investigated and the results are presented in Section 3.1. The results of the mixture of $LiAlH_4 + LiNH_2$ (Eq. (5)) are also reported in Section 3.2. In Section 3.3, the results of the dehydriding reaction of the mixture composed of other complex hydrides are reported. On the basis of these results, we identified the complex hydrides that should be mixed together for producing new pathways for the dehydriding reactions.

2. Experimental

The starting materials of $LiBH_4$, $LiAlH_4$ and $LiNH_2$ (95% purities) were purchased from Aldrich Co. Ltd. They were pre-mixed manually in the molar ratios of 1:2 (mixtures of

$LiBH_4 + 2LiNH_2$ and $LiAlH_4 + 2LiNH_2$) and 2:1 (mixture of $2LiBH_4 + LiNH_2$) using agate mortar and pestle. Then, parts of the samples were mechanically mixed by planetary ball milling (Fritsch P-7) with 20 steel balls (7 mm in diameter) in a hardened steel vial (30 cm^3 in volume) for 5 and 60 min under purified argon at 0.1 MPa. In order to avoid an increase in the temperature of the sample, the milling process was paused and rested every 15, respectively.

The samples thus prepared were examined by powder X-ray diffraction measurement (PANalytical X'PERT with Cu Kα radiation, the measurement time for each sample was 3.5 min), gas chromatography (GL Science GC323, argon flow rate of 40 ml min^{-1} and heating rate of 5 K min^{-1}), differential thermal analysis (Rigaku TG8120, helium flow rate of 150 ml min^{-1} and heating rate of 5 K min^{-1}) and mass spectroscopy (Anelva M-QA200TS, directly connected with the differential thermal analysis). The samples were handled in a glove box filled with purified argon or helium (the dew point for both was below 180 K). In the case of powder X-ray diffraction measurement, the sample on a glass plate, which was to be transferred to an X-ray diffractometer, was placed in a gas-tight container in order to minimise the effects of air. (It was confirmed that there was no significant difference in the diffraction profiles of the sample sealed by the Kapton-tape.) The gas-tight container equipped with gas exchanging and heating units was used for gas chromatography. The equipment for differential thermal analysis and mass spectroscopy was installed inside the glove box.

3. Results and discussion

3.1. Mixture of $LiBH_4 + 2LiNH_2$

3.1.1. Thermal desorption spectroscopy and structural change during the dehydriding process

Figs. 2 and 3 show the thermal desorption profiles (detected by gas chromatography) and powder X-ray diffraction profiles obtained after the thermal desorption, respectively. The following four samples: (a) $LiBH_4$, (b) $LiNH_2$, (c) the mixture of $2LiBH_4 + LiNH_2$ and (d) the mixture of $LiBH_4 + 2LiNH_2$ were manually prepared using agate mortar and pestle. A large desorption peak was observed at approximately 800 K during the dehydriding reaction of $LiBH_4$, as shown in Fig. 2(a). According to Eq. (1), the peaks of LiH [22] were detected in the powder X-ray diffraction profile after the dehydriding reaction, as shown in Fig. 3(a). The absence of any trace of B in the diffraction profile suggests that it is in an amorphous phase. $LiNH_2$ desorbs ammonia at approximately 600 K as follows:

$$LiNH_2 \rightarrow (1/2)Li_2NH + (1/2)NH_3$$
$$\rightarrow (1/3)Li_3N + (2/3)NH_3 \quad (7)$$

Li_2NH [23] was detected in the powder X-ray diffraction profile after a partial decomposition reaction, as shown in

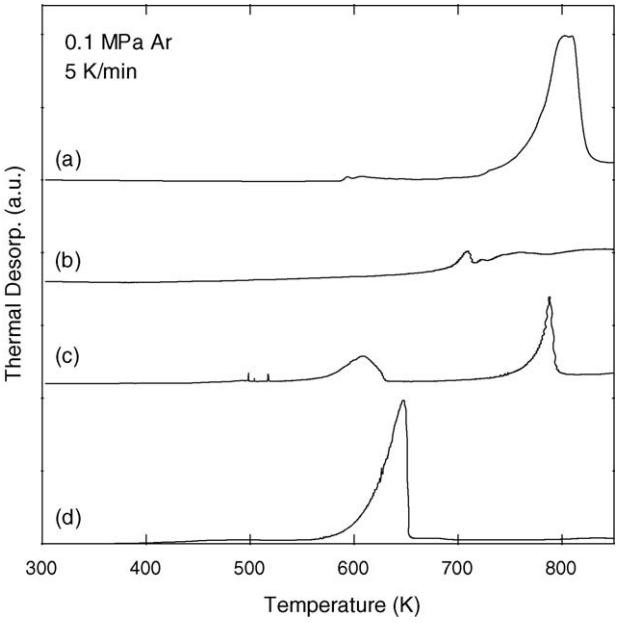

Fig. 2. Thermal desorption profiles for (a) $LiBH_4$, (b) $LiNH_2$, (c) the mixture of 2 $LiBH_4 + LiNH_2$, and (d) the mixture of $LiBH_4 + 2$ $LiNH_2$, detected by gas chromatography. Argon flow rate is 40 ml min^{-1}.

Fig. 3(b). There are broad and sharp thermal desorption peaks at approximately 600 and 800 K for the mixture of $2LiBH_4 + LiNH_2$, as shown in Fig. 2(c). The lower temperature peak probably corresponds to the dehydriding reaction of Eq. (4) and the higher peak corresponds to that of $LiBH_4$ alone, which is expressed in Eq. (1). Thus, the thermal desorption profile of the mixture of $2LiBH_4 + LiNH_2$ is expressed

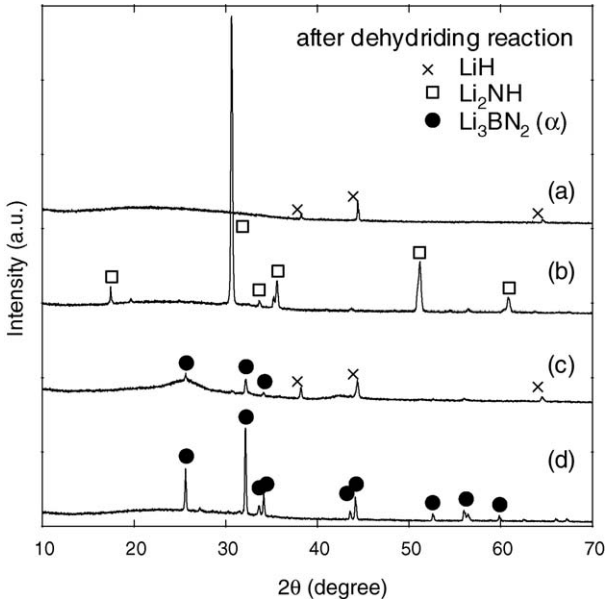

Fig. 3. Powder X-ray diffraction profiles of (a) $LiBH_4$, (b) $LiNH_2$, (c) the mixture of $2LiBH_4 + LiNH_2$, and (d) the mixture of $LiBH_4 + 2LiNH_2$ after the thermal desorption measurement. Crosses, opened squares, and closed circles denote the peak positions of LiH, Li_2NH and Li_3BN_2 (α) in [22–24], respectively.

as follows:

$$2LiBH_4 + LiNH_2 (= (1/2)(LiBH_4 + 2LiNH_2) + (3/2)LiBH_4) \rightarrow (1/2)(Li_3BN_2 + 4H_2) + (3/2)(LiH + B + (3/2)H_2) \quad (8)$$

In fact, the phases of Li_3BN_2 (α) [24] and LiH were observed in the sample after the dehydriding reaction, as shown in Fig. 3(c). (In this case also, the diffraction peak of B was absent.) Therefore, we expect that the quantity of $LiBH_4$ exceeds the required quantity in the mixture of $2LiBH_4 + LiNH_2$ for the single dehydriding reaction of Eq. (4). On the other hand, as shown in Fig. 2(d), the mixture of $LiBH_4 + 2LiNH_2$ exhibits a sharp thermal desorption peak at approximately 650 K, following the very small and broad thermal desorption peak below approximately 600 K. Further, the single phase of Li_3BN_2 (α) was detected in Fig. 3(d). These results confirm the occurrence of the dehydriding reaction of Eq. (4). It should be emphasized that the dehydriding temperature of the mixture of $LiBH_4 + 2LiNH_2$ is lower than that of $LiBH_4$ by approximately 150 K. In other words, we can destabilise the dehydriding reaction of $LiBH_4$ by producing a new pathway in the reaction with 2 M of $LiNH_2$.

The structural change in the mixture of $LiBH_4 + 2LiNH_2$ (Eq. (4) and Fig. 2(d)) with an increase in temperature was investigated by powder X-ray diffraction measurement, and the results are shown in Fig. 4. Upon heating, four phases: (i) $LiBH_4 + 2LiNH_2$ [25,26] (starting material); (ii) $Li_3BN_2H_8$ [27] (373–573 K); (iii) Li_3N–BN [28] + $4H_2$ (573–773 K); (iv) Li_3BN_2 (α) [24] + $4H_2$ (873 K), were formed sequentially. The phases of $Li_3BN_2H_8$ and Li_3N–BN appear at a temperature before and after the sharp thermal desorption peak shown in Fig. 2(d), respectively. Recently, it was reported that the crystal structure of $Li_3BN_2H_8$ is body-centered cubic with lattice constant of $a = 1.076$ nm [27]. Further, Li_3N–BN has been reported as a quenched phase of the mixture of $Li_3N + BN$ resulting from high pressure [28], which was also denoted as Li_3BN_2 (W) in [29]. (Their X-ray diffraction data are essentially similar, and the product Li_3N–BN is a compound and not a mixture. In this paper, we use the description of 'Li_3N–BN' based on the description in the JCPDS-ICDD database, 00-013-0393.) However, since the precise crystal structures of $Li_3BN_2H_8$ and Li_3N–BN have not been clarified till date, we have investigated the crystal structure by synchrotron radiation X-ray diffraction measurement [30]. The preliminary results indicate that $Li_3BN_2H_8$ crystallizes in a cubic symmetry (space group: *Im*-3) with a lattice constant $a = 1.067$ nm, which is composed of Li^+ and two types of anions, $[BH_4]^-$ and $[NH_2]^-$. On the other hand, Li_3N–BN has a tetragonal structure (space group: $I4_1md$) with the lattice constants of $a = 0.6583$ nm and $c = 1.0326$ nm, which is composed of Li^+ and an anion $[N–B–N]^{3+}$, such as Li_3BN_2 (α) [24]. The precise structure will be reported in detail elsewhere [30].

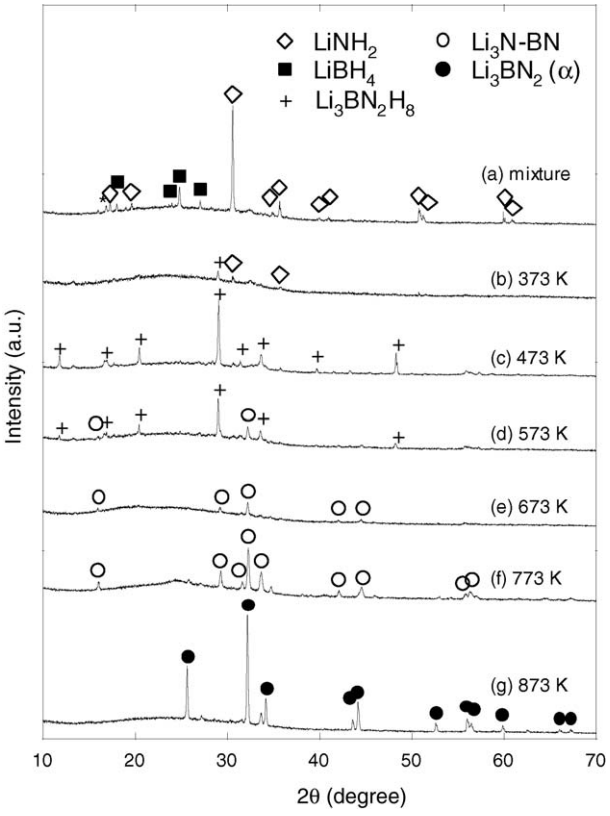

Fig. 4. Powder X-ray diffraction profiles of the mixture of $LiBH_4 + 2LiNH_2$ under various heating temperatures. Opened diamonds, closed squires, pluses, opened circles and closed circles denote the peak positions of $LiNH_2$, $LiBH_4$, $Li_3BN_2H_8$, Li_3N–BN and Li_3BN_2 (α) in [25–28] and [24], respectively. Asterisk in the profile (a) shows the peak position of small quantity of the impurity phase ($Li_2B_2O_4$ or LiB_3O_5).

3.1.2. *Effects of milling on the dehydriding process*

Thus far, ball milling has been reported to be effective for the promotion of the dehydriding reaction of the mixture of $LiNH_2 + LiH$ [31]. Therefore, in the present study, we have also applied ball milling to the mixture of $LiBH_4 + 2LiNH_2$. The thermal desorption profiles (detected by gas chromatography) of the two types of mixtures, which were manually pre-mixed and mechanically mixed by ball milling (5 and 60 min), are shown in Fig. 5. The profiles are unexpectedly observed to be fairly similar to each other. This property is completely different from the cases of the mixtures of $LiNH_2 + LiH$ [31] and $LiAlH_4 + 2LiNH_2$ (described in the next section). As shown in the inset, $Li_3BN_2H_8$ was observed in the mixture after milling for both 5 and 60 min. The diffraction peaks of $Li_3BN_2H_8$ shift to a higher angle with an increase in the milling time, thereby indicating a reduction in hydrogen concentration. In fact, the quantities of desorbed hydrogen estimated from the peak areas in Fig. 5 decrease with an increase in milling time (9.5 mass% (pre-mixed manually), 9.0 mass% (mechanically mixed by ball milling for 5 min) and 7.9 mass% (mechanically mixed by ball milling for 60 min)).

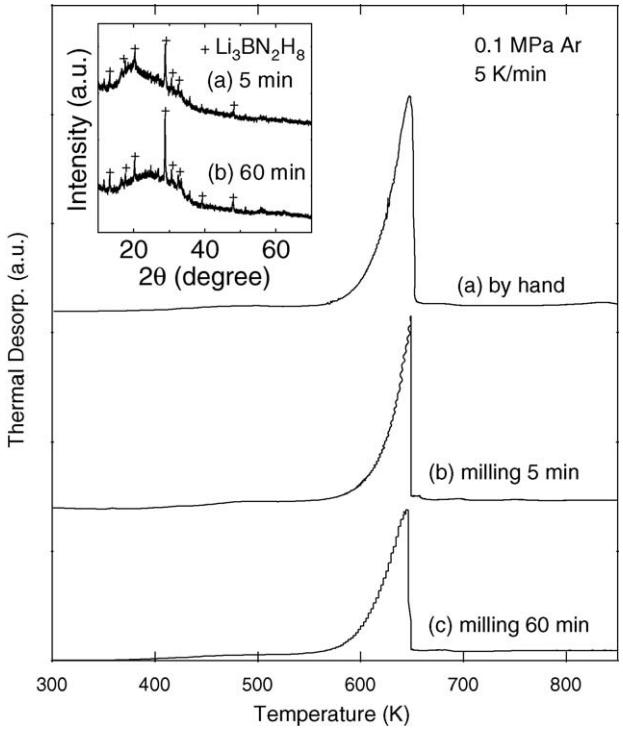

Fig. 5. Thermal desorption profiles of the mixture of $LiBH_4 + 2LiNH_2$: (a) manually pre-mixed and mechanically mixed by planetary ball milling for (b) 5 min and (c) 60 min. Argon flow rate is 40 ml min^{-1}. The inset shows the powder X-ray diffraction profiles of the mixture of $LiBH_4 + 2LiNH_2$ after milling for 5 and 60 min. Pluses show the peak positions of $Li_3BN_2H_8$ (refer the text).

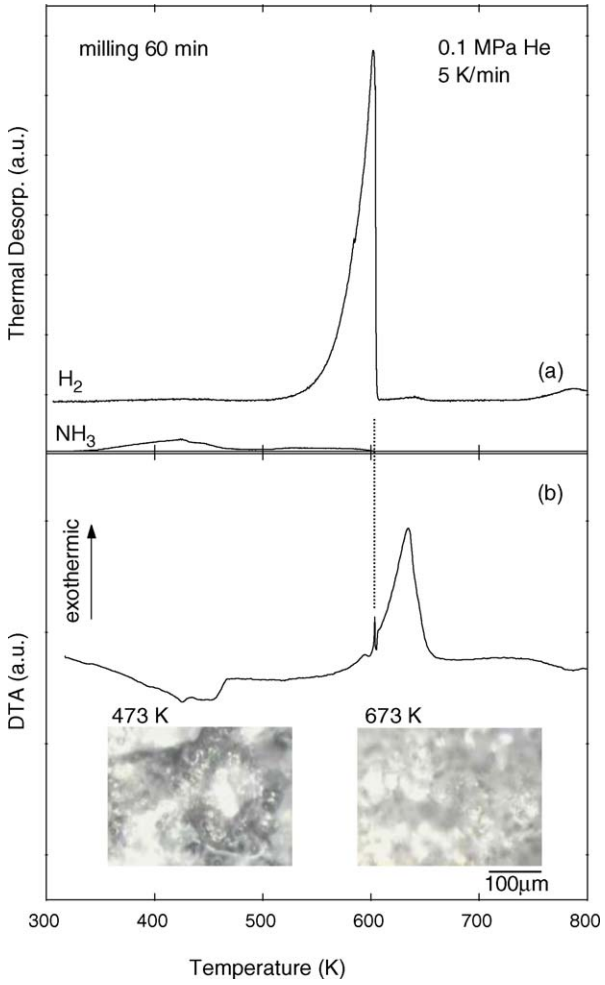

Fig. 6. (a) Thermal desorption profile detected by mass-spectroscopy, and (b) differential thermal analysis of the mixture of $LiBH_4 + 2LiNH_2$ mechanically mixed by planetary ball milling for 60 min. Helium flow rate is 150 ml min^{-1}. Surface morphology changes by melting and solidification reactions of the mixture were observed using an in situ microscope equipped with a CCD camera under argon atmosphere; their micrographs at 473 K (during melting) and 673 K (after solidification) are shown in inset.

The components of the desorbed gas are investigated by mass spectroscopy and the result of the mixture that was mechanically mixed by ball milling for 60 min, is shown in Fig. 6(a). (The differences in the peak temperatures between the thermal desorption profiles detected by gas chromatography (Fig. 5(c)) and those by mass spectroscopy (Fig. 6(a)) arise due to different conditions of the heating atmospheres and gas flow rates.) We observe that the desorbed gas components of the small and broad desorption peak below 500 K contain ammonia, while the component of the sharp desorption peak at approximately 600 K is dominantly hydrogen. A similar tendency was also observed in the samples that were manually pre-mixed and mechanically mixed by ball milling for 5 min.

As shown in Fig. 6(b), the endothermic and exothermic peaks were detected at approximately 350–450, 600–650 K, respectively. The former corresponds to the small and broad desorption peak in Fig. 6(a), while the latter appears at a slightly higher (approximately 35 K) temperature of the main dehydriding peak in Fig. 6(a). The enthalpy of the main dehydriding reaction has been predicted to be endothermic by the first-principles calculations (ΔH of the dehydriding reaction is 23 kJ mol^{-1} H_2) [16], whereas the experimental result shows a large exothermic peak (ΔH of the dehydriding reaction is negative, i.e. the dehydriding phase is more stable than the hydriding phase if the exothermic peak at approximately 600–650 K originates from the dehydriding reaction). The possible explanations for this inconsistency are as follows: $Li_3BN_2H_8$ melts at 473 K, and then, the product (i.e. Li_3N–BN) solidifies at 673 K after the dehydriding reaction, as shown in inset of Fig. 6(b). Thus, the exothermic peak might have originated from the latent heat of solidification of Li_3N–BN after the dehydriding reaction and not due to the actual dehydriding reaction. Another explanation is the difference between the actual reaction and Eq. (4) using calculation. Further, theoretical and experimental investigations are required in order to clarify the intrinsic origin of the exothermic peak shown in Fig. 6(b).

Attempts are being made to achieve the rehydriding (absorbing) reaction and to avoid ammonia desorption by the addition of catalysts, application of long-term milling and optimisation of the compositions.

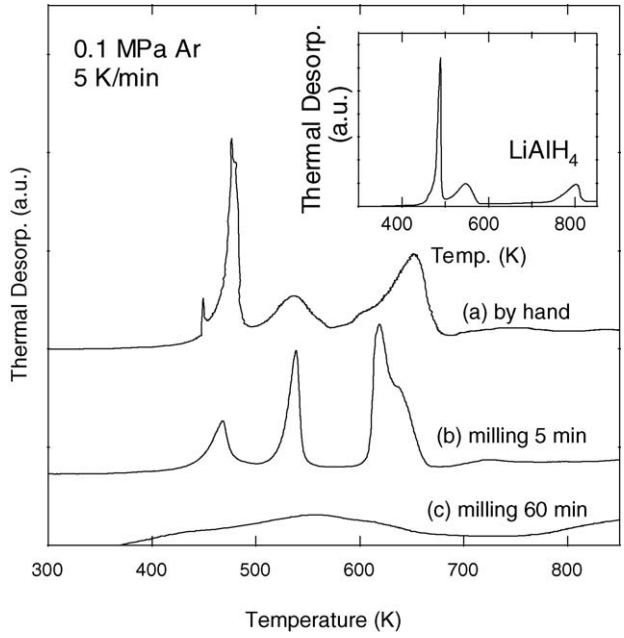

Fig. 7. Thermal desorption profiles of the mixture of $LiAlH_4 + 2\,LiNH_2$: (a) manually pre-mixed and mechanically mixed by planetary ball milling for (b) 5 min and (c) 60 min, detected by gas chromatography. Argon flow rate is 40 ml min^{-1}. Inset shows the profile of $LiAlH_4$ alone, as a reference.

3.2. Mixture of $LiAlH_4 + 2LiNH_2$

3.2.1. Thermal desorption spectroscopy and structural change during the dehydriding process

Fig. 7 shows the thermal desorption profiles (detected by gas chromatography) of the mixture of $LiAlH_4 + 2LiNH_2$ that was (a) manually pre-mixed and mechanically mixed by ball milling for (b) 5 min and (c) 60 min. The profile of $LiAlH_4$ alone is also shown in the inset as a reference. In this profile, there are three desorption peaks, one sharp and two broad peaks at approximately 490, 550 and 800 K. The desorption peaks at approximately 490 and 550 K correspond to the dehydriding reaction of the two-step reactions of Eq. (2), and the desorption peak at approximately 800 K corresponds to the dehydriding reaction of the right hand term of Eq. (2), i.e. from 'LiH + Al' to 'LiAl' [2]. Three desorption peaks are also observed in the mixture of $LiAlH_4 + 2LiNH_2$ that was pre-mixed manually. The two desorption peaks at approximately 490 and 550 K are similar to those of $LiAlH_4$ alone, while the peak at a higher temperature (approximately 650 K) shifts to a lower temperature as compared to that of $LiAlH_4$ alone. The desorption reaction at approximately 650 K in Fig. 7(a) appears to occur due to the dehydriding reaction of the mixture of LiH (formed by the dehydriding reaction of $LiAlH_4$) + $LiNH_2$, which is similar to the dehydriding reaction of Eq. (3). Three thermal desorption peaks are also observed for the mixture of $LiAlH_4 + 2LiNH_2$ mixed by ball milling for 5 min, whereas the desorption peak at the lower temperature becomes smaller. The results of mass spectroscopy suggested that the components of the desorbed gases in the mixtures of $LiAlH_4 + 2LiNH_2$ pre-mixed manually and mixed by ball milling for 5 min (not shown) are not only hydrogen but also ammonia. These results indicate that the reactions of Eqs. (2), (3) and (7) proceed in the mixtures of $LiAlH_4 + 2LiNH_2$ that is manually pre-mixed and mechanically mixed by ball milling for 5 min. On the other hand, as shown in Fig. 7(c), a broad desorption peak begin to appear at approximately 370 K for the mixture of $LiAlH_4 + 2LiNH_2$ mixed by ball milling for 60 min. The quantity of desorbed hydrogen estimated from the peak area in Fig. 7(c) is 4.1 mass%, which is smaller than the ideal value obtained from Eq. (5). The results of mass spectroscopy confirm that only hydrogen and not ammonia was detected as the components of desorbed gas in the mixture of $LiAlH_4 + 2LiNH_2$ mixed by ball milling for 60 min, as shown in the Fig. 8(a). Moreover, as shown in inset of Fig. 8(a), very small and broad X-ray diffraction peaks of Li_3AlN_2 were observed after the thermal desorption reaction. From these results, the dehydriding reaction of Eq. (5) proceeds with the mixture of $LiAlH_4 + 2LiNH_2$ mixed by ball milling for 60 min, and the partial dehydriding reaction occurs earlier during ball milling.

It should be emphasized that the dehydriding reaction of the mixture of $LiAlH_4 + 2LiNH_2$ is endothermic, while that of $LiAlH_4$ is rather complicated but is essentially exothermic, as shown in Fig. 8(b). Since the rehydriding reaction proceeds easily, an endothermic dehydriding reaction is desired for hydrogen storage. We can control the stability of the dehydriding reaction of $LiAlH_4$ from exothermic to endothermic by producing a new pathway by mixing 2 M of $LiNH_2$.

3.2.2. Comparison of the effects of milling on the dehydriding process for the mixture of $LiBH_4 + 2LiNH_2$

The reaction pathway for the mixture of $LiAlH_4 + 2LiNH_2$ (Fig. 7) evidently depends on the milling conditions, while there are no major effects of milling on the mixture of $LiBH_4 + 2LiNH_2$ (Fig. 5). In this section, we briefly discuss the different milling effects.

As mentioned earlier, the mixture of $LiBH_4 + 2LiNH_2$ changes to $Li_3BN_2H_8$ by heating (373 K) or by mechanical milling (5 min). Upon heating, $Li_3BN_2H_8$ melts at 463 K [28]. The dehydriding reaction then proceeds in the liquid phase at higher temperatures. The reaction has been visually confirmed by microscopic observations, as shown in Fig. 9(a). Therefore, there is no significant effect of milling on the mixture of $LiBH_4 + 2LiNH_2$. On the other hand, the mixture of $LiAlH_4 + 2LiNH_2$ does not melt up to 873 K, and the dehydriding reaction proceeds in the solid phase, as shown in Fig. 9(b). During the dehydriding reaction, the sample was partially separated, which may be due to the difference in the density of the sample before and after the dehydriding reaction. Therefore, sufficient contact between $LiAlH_4$ and $LiNH_2$ is essential for the dehydriding reaction.

Attempts are being made to increase the quantity of stored hydrogen and to achieve the rehydriding reaction for the

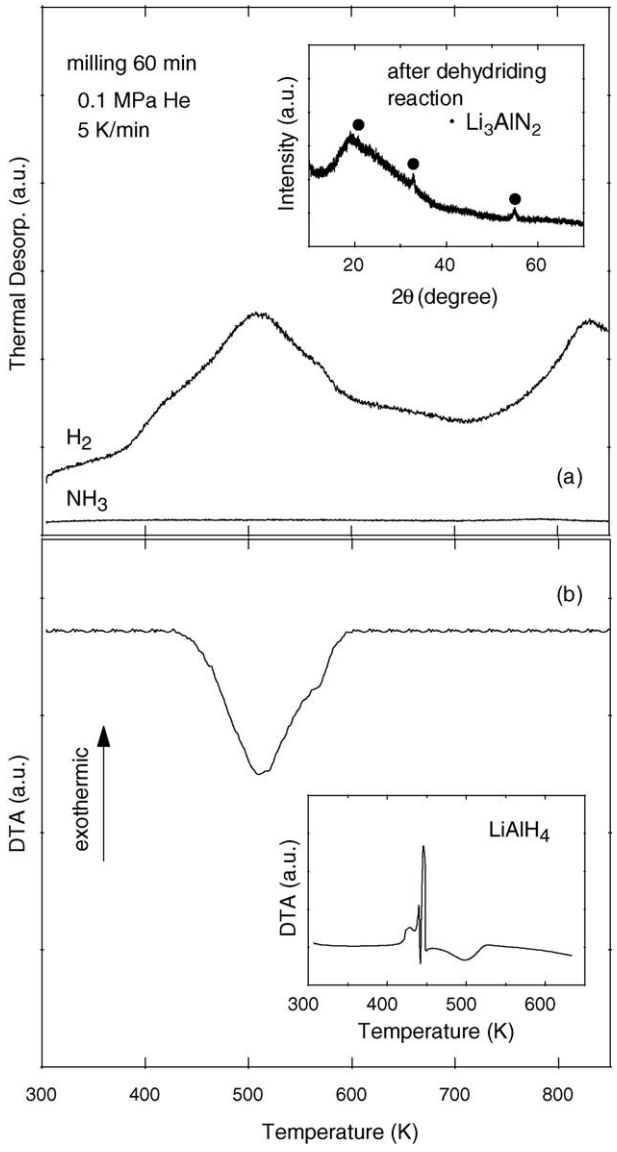

Fig. 8. (a) Thermal desorption profile detected by mass-spectroscopy and (b) differential thermal analysis of the mixture of $LiAlH_4 + 2LiNH_2$ mechanically mixed by planetary ball milling for 60 min. The atmosphere is helium flow with heating rate of 150 ml min^{-1}. Powder X-ray diffraction profile of the mixture of $LiAlH_4 + 2LiNH_2$ after the dehydriding reaction are shown in inset of (a). Closed circles denote the peak positions of Li_3AlN_2 [32]. Inset of (b) shows the result of differential thermal analysis of $LiAlH_4$.

mixture of $LiAlH_4 + 2LiNH_2$ by using a high-pressure gas reaction unit [33].

3.3. Proposal on new pathways for dehydriding reactions

On the basis of the results of some other mixtures, we will identify the complex hydrides that should be mixed together to produce new pathways for dehydriding reactions.

Fig. 10 shows the thermal desorption profiles of the mixture of $MBH_4 + 2LiNH_2$ (M = Li, Na, K) that was mechanically mixed by ball milling for 60 min

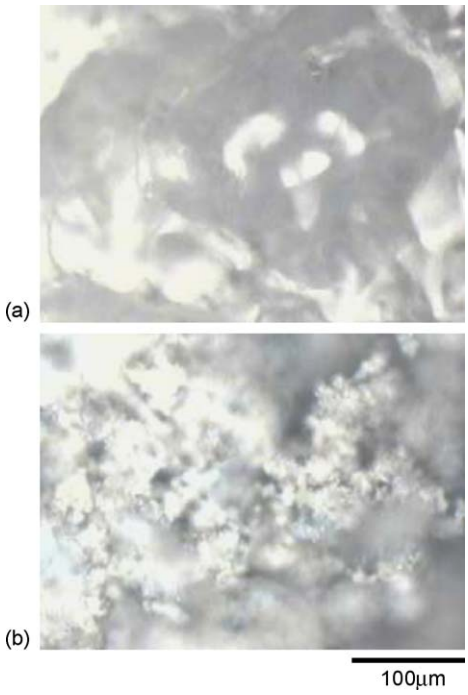

Fig. 9. Micrographs of (a) the mixture of $LiBH_4 + 2LiNH_2$ at 573 K and (b) the mixture of $LiAlH_4 + 2LiNH_2$ at 523 K, which were observed using an in situ microscope equipped with a CCD camera under argon atmosphere. The dehydriding reactions were proceed in the liquid state for the mixture of $LiBH_4 + 2LiNH_2$ and solid states for the mixture of $LiAlH_4 + 2LiNH_2$, respectively.

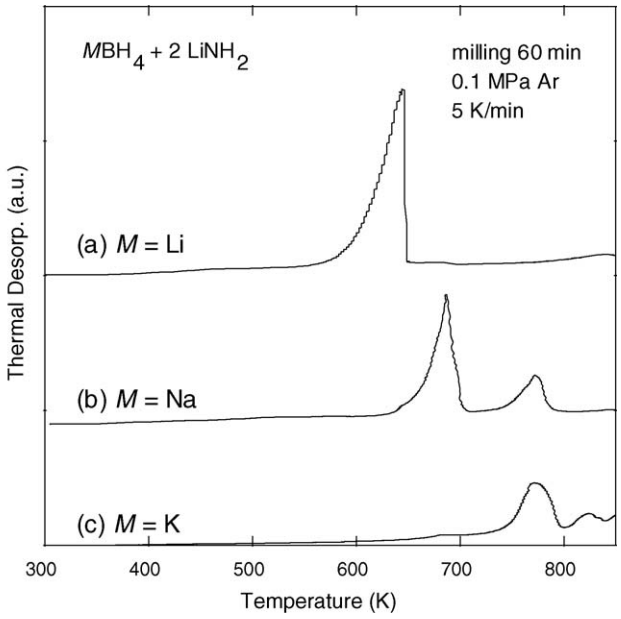

Fig. 10. Thermal desorption profiles of the mixture of $MBH_4 + 2LiNH_2$ (M = Li, Na, K) that was mechanically mixed by planetary ball milling for 60 min, detected by gas chromatography. Argon flow rate is 40 ml min^{-1}.

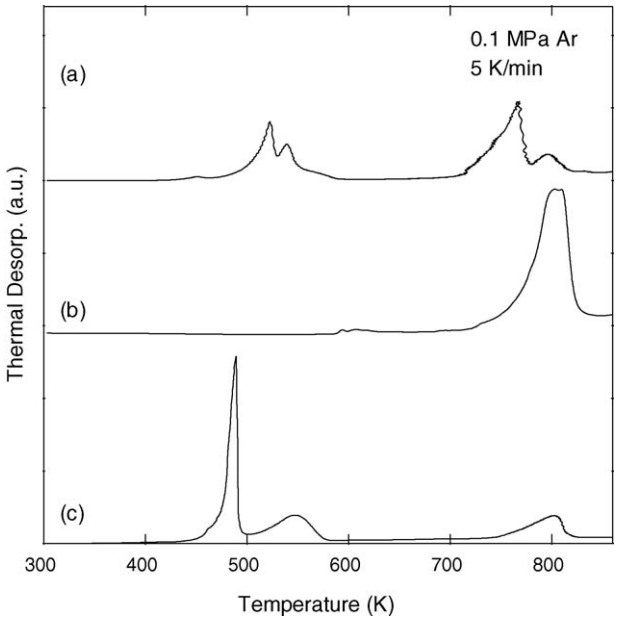

Fig. 11. Thermal desorption profiles of (a) the mixture of $LiBH_4 + LiAlH_4$ mechanically mixed by planetary ball milling for 60 min (b) $LiBH_4$ and (c) $LiAlH_4$, detected by gas chromatography. Argon flow rate is 40 ml min^{-1}.

(detected by gas chromatography). The thermal desorption peaks shift to higher temperatures in the order of $LiBH_4 < NaBH_4 < KBH_4$. The melting and dehydriding temperatures (T_m and T_d) are also increased in the same order as $LiBH_4$ ($T_m = 541$ K, $T_d = 653$ K) < $NaBH_4$ ($T_m = 778$ K, $T_d = 838$ K) < KBH_4 ($T_m \sim T_d = 858$ K) [34]. Similarly, the dehydriding temperature of the mixture of $LiBH_4 + 2LiNH_2$ is higher than that of $LiAlH_4 + 2LiNH_2$ and both T_m and T_d of $LiBH_4$ are higher than those of $LiAlH_4$. Therefore, one of the criteria for selecting complex hydrides is the melting and dehydriding temperatures; lower temperatures are highly advantageous.

The thermal desorption profiles of the mixture of $LiBH_4 + LiAlH_4$, which was mechanically mixed by ball milling for 60 min (detected by gas chromatography), are shown in Fig. 11(a). The results of $LiBH_4$ and $LiAlH_4$ are also shown in Fig. 11(b) and (c) as references. By considering the first criterion, $LiAlH_4$ is a suitable complex hydride for one of the components because both T_m and T_d are sufficiently low. However, the dehydriding reaction of the mixture of $LiBH_4 + LiAlH_4$ is completely separated into those of $LiBH_4$ and $LiAlH_4$. This is because no stable product is formed after the dehydriding reaction (e.g. Li_2BAl does not exist). Thus, the dehydriding reactions of $LiBH_4$ and $LiAlH_4$ proceed separately. A similar reaction was also observed in the mixture of $2LiBH_4 + LiNH_2$ (Fig. 2(c)) in which hydrogen was also desorbed by a large quantity of $LiBH_4$ at only the dehydriding temperature of $LiBH_4$. Therefore, another criterion for selecting complex hydrides is the existence of products after the dehydriding reactions; the existence of stable phases is required.

On the basis of the two criteria described above and the theoretical calculations, new pathways are being explored for efficient development of mixed complex hydrides. In addition to complex hydrides, production of new pathways for other hydrides, such as '$LiBH_4 + (1/2)MgH_2$ [35]', '$4LiH/2MgH_2 + Si$ [36]' and '$AlH_3 + LiH/MgH_2$ [37]', has also been reported.

4. Conclusions

In the present study, the following new pathways for the dehydriding reactions of mixed complex hydrides were confirmed: $LiBH_4 + 2LiNH_2 \rightarrow Li_3BN_2 + 4H_2$ and $LiAlH_4 + 2LiNH_2 \rightarrow Li_3AlN_2 + 4H_2$. In these reactions, 11.9 and 9.6 mass% of hydrogen can be desorbed theoretically. The quantities of desorbed hydrogen were experimentally deduced as approximately 7.9–9.5 and 4.1 mass% for the mixtures of $LiBH_4 + 2LiNH_2$ and $LiAlH_4 + 2LiNH_2$, respectively. The dehydriding reaction of $LiBH_4$ proceeds at approximately 800 K, while that of the mixture of $LiBH_4 + 2LiNH_2$ proceeds at approximately 650 K. This indicates that the dehydriding temperature of $LiBH_4$ reduces by 150 K by mixing 2 M of $LiNH_2$. The exothermic peak was observed at a slightly higher temperature of the dehydriding reaction of the mixture of $LiBH_4 + 2LiNH_2$. However, the peak may be due to the solidification of the product and not due to the exothermic dehydriding reaction of the mixture itself. Although the first-step dehydriding reaction of $LiAlH_4$ is exothermic, the mixture of $LiAlH_4 + 2LiNH_2$ exhibits an endothermic dehydriding reaction. These results suggest that the stability of the dehydriding reactions of complex hydrides can be controlled by producing new pathways by mixing. We propose two criteria for producing new pathways: One criterion is to select complex hydrides with lower melting/dehydriding temperatures and the other is to select them on the basis of the products formed after the dehydriding reactions.

Acknowledgements

The authors would like to acknowledge Dr. S. Towata for valuable discussion. This work is partially supported: by the Ministry of Education, Culture, Sports, Science and Technology, "Grant-in-Aid for Encouragement of Young Scientists (B), #17760555 (A), #15686027"; by the New Energy and Industrial Technology Development Organization (NEDO), "Development of Safe Utilization Technology and an Infrastructure for Hydrogen Use (2003-2005), #03001387"; by the Thermal and Electric Energy Technology Foundation; by the Hayashi Memorial Foundation for Female Natural Scientists; by the Intelligent Cosmos Academic Foundation; by the Collaborative Research in Center for Interdisciplinary Research, Tohoku University.

References

[1] A. Züttel, S. Rentsch, P. Fisher, P. Wenger, P. Sudan, Ph. Mauron, Ch. Emmenegger, J. Power Sources 118 (2003) 1–7;
A. Züttel, S. Rentsch, P. Fisher, P. Wenger, P. Sudan, Ph. Mauron, Ch. Emmenegger, J. Alloys Compd. 356–357 (2003) 515–520.

[2] L. Zaluski, A. Zaluska, J.O. Ström-Olsen, J. Alloys Compd. 290 (1999) 71–78;
V.P. Balema, V.K. Pecharsky, K.W. Dennis, J. Alloys Compd. 313 (2000) 69–74.

[3] S. Suda, Y.-M. Sun, B.-H. Liu, Y. Zhou, S. Morimitsu, K. Arai, N. Tshukamoto, M. Uchida, Y. Candra, Z.-P. Li, Appl. Phys. A 72 (2001) 209–212.

[4] Y. Kojima, K. Suzuki, K. Fukumoto, M. Sasaki, T. Yamamoto, Y. Kawai, H. Hayashi, Int. Hydrogen Energy 27 (2002) 1029–1034.

[5] V.P. Balema, J.W. Wiench, K.W. Dennis, M. Pruski, V.K. Pecharsky, J. Alloys Compd. 329 (2001) 108–114.

[6] J. Chen, N. Kuriyama, Q. Xu, H.T. Takeshita, T. Sakai, J. Phys. Chem. B 105 (2001) 11214–11220.

[7] B. Bogdanović, M. Schwickardi, J. Alloys Compd. 253 (1997) 1–7; B. Bogdanović, M. Schwickardi, Appl. Phys. A 72 (2001) 221–223.

[8] R.A. Zidan, S. Takara, A.G. Hee, C.M. Jensen, J. Alloys Compd. 285 (1999) 119–122.

[9] K.J. Gross, S. Guthrie, S. Takara, G. Thomas, J. Alloys Compd. 297 (2000) 270–281.

[10] H. Morioka, K. Kakizaki, S.C. Chung, A. Yamada, J. Alloys Compd. 353 (2003) 310–314.

[11] F.W. Dafert, R. Miklauz, Monatsh. Chem. 31 (1910) 981–993.

[12] P. Chen, Z. Xiong, J. Luo, J. Lin, K.L. Tan, Nature 420 (2002) 302–304.

[13] O. Ruff, H. Goeres, Chem. Ber. 44 (1911) 502–506;
P. Chen, Z. Xiong, J. Luo, J. Lin, K.L. Tan, J. Phys. Chem. B 107 (2003) 10967–10970;
T. Ichikawa, S. Isobe, N. Hanada, H. Fujii, J. Alloys Compd. 365 (2004) 271–276.

[14] C.D. Montgomery, Nucl. Eng. Des. 25 (1973) 309–314.

[15] M.B. Smith, G.E. Bass Jr., J. Chem. Eng. Data 8 (1963) 8.

[16] M. Aoki, K. Miwa, T. Noritake, G. Kitahara, Y. Nakamori, S. Orimo, S. Towata, Appl. Phys. A 80 (2005) 1409–1412.

[17] D. Vanderbilt, Phys. Rev. B 41 (1990) 7892–7895;
K. Laasonen, A. Pasquarello, R. Car, C. Lee, D. Vanderbilt, Phys. Rev. B 47 (1993) 10142–10153.

[18] P. Hohenberg, W. Kohn, Phys. Rev. 136 (1964) B864–B871;
W. Kohn, L.J. Sham, Phys. Rev. 470 (1965) A1133–A1138.

[19] J.P. Perdew, K. Burke, M. Ernzerhof, Phys. Rev. Lett. 77 (1996) 3865–3868;
J.P. Perdew, K. Burke, M. Ernzerhof, Phys. Rev. Lett. 78 (1997) 1396.

[20] K. Miwa, N. Ohba, S. Towata, Y. Nakamori, S. Orimo, Phys. Rev. B 69 (2004) 245120(1)–245120(8).

[21] R. Griessen, T. Riesterer, L. Schlapbach (Eds.), Hydrogen Intermetallic Compd. I (1988) 266.

[22] R.S. Calder, W. Cochran, D. Griffiths, R.D. Lowde, J. Phys. Chem. Solid 23 (1962) 621–632.

[23] K. Ohoyama, Y. Nakamori, S. Orimo, K. Yamada, J. Phys. Soc. Jpn. 74 (2005) 483–487;
T. Noritake, H. Nozaki, M. Aoki, S. Towata, G. Kitahara, Y. Nakamori, S. Orimo, J. Alloys Compd. 393 (2005) 264–268.

[24] H. Yamane, S. Kikkawa, M. Koizumi, J. Solid State Chem. 71 (1987) 1–11.

[25] J.-Ph. Soulié, G. Renaudin, R. Cerny, K. Yvon, J. Alloys Compd. 346 (2002) 200–205.

[26] V.R. Juza, K. Opp, Z. Anorg. Allg. Chem. 266 (1951) 313–324.

[27] F.E. Pinkerton, G.P. Meisner, M.S. Meyer, M.P. Balogh, M.D. Kundrat, Phys. Chem. B 109 (2005) 6–9.

[28] R.H. Wentorf Jr., J. Phys. Chem. 34 (1961) 809–812.

[29] R.C. DeVries, J.F. Fleischer, Mat. Res. Bull. 4 (1969) 433–442.

[30] T. Noritake et al., in preparation.

[31] T. Ichikawa, S. Isobe, N. Hanada, H. Fujii, J. Alloys Compd. 356 (2004) 271–276.

[32] V.R. Juza, F. Hund, Z. Anorg. Chem. 257 (1948) 13–25.

[33] Y. Nakamori, S. Orimo, Mater. Sci. Eng. B 108 (2004) 48–50.

[34] S. Orimo, Y. Nakamori, Züttel, Mater. Sci. Eng. B 108 (2004) 51–53.

[35] M. Au, J. Holder, T. Motyka, J.J. Vajo, S.L. Skeith, F. Mertens, Presented in ASM 2004 MRS Meeting, 2004.

[36] J.J. Vajo, F. Mertens, C.C. Alm, R.C. Bowman, B. Fultz, J. Phys. Chem. B 108 (2004) 13977–13983.

[37] G. Sandrock, J. Reilly, J. Graetz, W.-M. Zhou, J. Johnson, J. Wegrzyn, Appl. Phys. A 80 (2005) 687–690.